

**Critical Role of Water Content in the Formation and Reactivity of Uranium, Neptunium, and Plutonium Iodates Under Hydrothermal Conditions: Implications for the Oxidative Dissolution of Spent Nuclear Fuel**

Travis H. Bray,<sup>1</sup> Jie Ling,<sup>1</sup> Eun-Sang Choi,<sup>2</sup> James S. Brooks,<sup>2</sup> James V. Beitz,<sup>3</sup>

Richard E. Sykora,<sup>4</sup> Richard G. Haire,<sup>5</sup> David M. Stanbury,<sup>1</sup> and Thomas E. Albrecht-Schmitt<sup>1,\*</sup>

<sup>1</sup>Department of Chemistry and Biochemistry and E. C. Leach Nuclear Science Center, Auburn University, Auburn, Alabama 36849

<sup>2</sup>Department of Physics and National High Magnetic Field Laboratory, Florida State University, Tallahassee, Florida 32310

<sup>3</sup>Chemistry Division, Argonne National Laboratory, Argonne, Illinois 60439

<sup>4</sup>Department of Chemistry, University of South Alabama, Mobile, Alabama 36688

<sup>5</sup>Chemical Sciences Division, Transuranium Research Laboratory, Oak Ridge National Laboratory, MS 6375, Oak Ridge, Tennessee 37831

A submission to *Science* as a Report

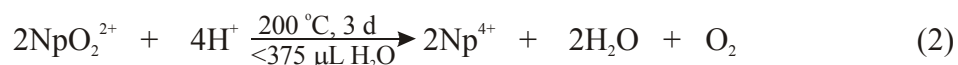
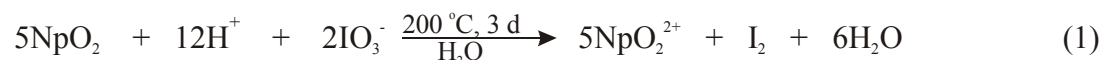
## Abstract

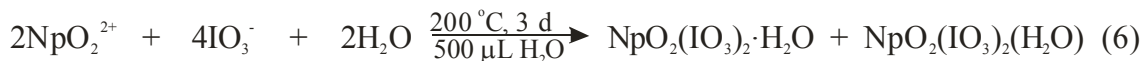
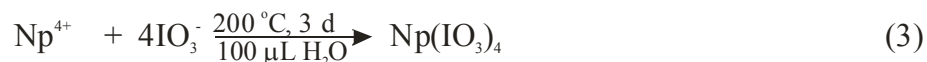
The reactions of  $^{237}\text{NpO}_2$  with excess iodate under acidic hydrothermal conditions result in the isolation of the Np(IV), Np(V), and Np(VI) iodates,  $\text{Np}(\text{IO}_3)_4$ ,  $\text{Np}(\text{IO}_3)_4 \cdot n\text{H}_2\text{O}$ ,  $\text{NpO}_2(\text{IO}_3)$ ,  $\text{NpO}_2(\text{IO}_3)_2(\text{H}_2\text{O})$ , and  $\text{NpO}_2(\text{IO}_3)_2 \cdot \text{H}_2\text{O}$ , depending on both the pH and the amount of water present in the reactions. Reactions with less water and lower pH favor reduced products. The prolonged hydrothermal reaction (30 days) of the Np(VI) iodates in the presence of iodate results in the reduction of Np(VI) to Np(IV), and the crystallization of  $\text{Np}(\text{IO}_3)_4$  and  $\text{Np}(\text{IO}_3)_4 \cdot n\text{H}_2\text{O}$ . While the initial redox processes involved in the reactions between  $^{237}\text{NpO}_2$  or  $^{242}\text{PuO}_2$  and iodate are similar, the low solubility of  $\text{Pu}(\text{IO}_3)_4$  dominates product formation in Pu iodate reactions to a much greater extent than  $\text{Np}(\text{IO}_3)_4$  does in the Np iodate system.  $\text{UO}_2$  reacts with iodate under these conditions to yield U(VI) iodates solely. The isotopic structures of the An(IV) iodates,  $\text{An}(\text{IO}_3)_4$  (An = Np, Pu) are reported, and consist of one-dimensional chains of dodecahedral An(IV) cations bridged by iodate anions. Single crystal magnetic susceptibility measurements of  $\text{Np}(\text{IO}_3)_4$  show magnetically isolated Np(IV) ions.

## Report

Under the oxidizing conditions present in the groundwater taken from wells near Yucca mountain, introduced iodine should occur in the form of both iodide,  $\text{I}^-$ , and iodate,  $\text{IO}_3^-$  (1). Whereas  $\text{I}^-$  is not expected to form strong complexes with actinide ions in aqueous media (2),  $\text{IO}_3^-$  forms stable, inner-sphere complexes with actinides (3). The remarkable insolubility of actinide iodates has been used for decades to precipitate actinides selectively from fission products and other elements (4). The initial form of actinides in spent nuclear fuel (SNF) is primarily the reduced forms, i.e.  $\text{UO}_2$ ,  $\text{NpO}_2$ , and  $\text{PuO}_2$ . Owing to its high vapor pressure, iodine is expected to be concentrated near the surface and in grain boundaries in SNF where it could react with dissolved oxygen in water to form iodate (5). Therefore, the products of the reactions of tetravalent actinides with iodate might play an important role in the potential release of several key long-lived radionuclides (e.g.  $^{129}\text{I}$ ,  $t_{1/2} = 1 \times 10^7$  y;  $^{238}\text{U}$ ,  $t_{1/2} = 4.46 \times 10^9$  y;  $^{237}\text{Np}$ ,  $t_{1/2} = 2.14 \times 10^6$  y, and  $^{239}\text{Pu}$ ,  $t_{1/2} = 2.411 \times 10^4$  y) into the environment in the event of aged SNF contacting groundwater. During the lifetime of stored SNF, it is possible that minute cracks and pores will form in the casing. This scenario will significantly limit the amount of groundwater interacting with the nuclear waste. Herein, we show that the chemistry that occurs under hydrothermal conditions where a limited amount of water is present is dramatically different from what is predicted based on traditional homogeneous solution chemistry (6).

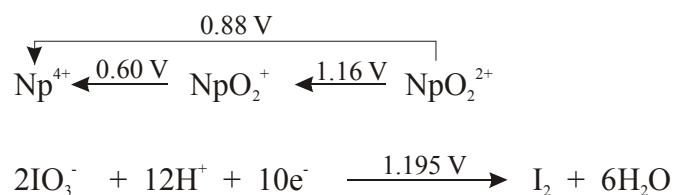
When  $^{237}\text{NpO}_2$  is reacted with excess iodate under acidic mild hydrothermal conditions,  $\text{Np(IV)}$ ,  $\text{Np(V)}$ , and  $\text{Np(VI)}$  iodates are isolated as is shown in Scheme 1 (7).





**Scheme 1.**

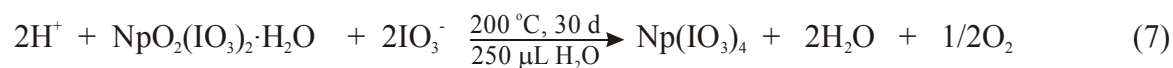
Reaction 1 describes the direct two-electron oxidation of  $\text{Np}^{4+}$  to  $\text{NpO}_2^{2+}$  by iodate. Acidic dissolution of  $\text{NpO}_2$  in the presence of oxygen typically yields  $\text{Np(V)}$  in the form of  $\text{NpO}_2^+$  in solution (e.g. in 1 M HCl). Reaction 1 is governed by the strong oxidizing potential of iodate under acidic conditions that is sufficient to directly oxidize  $\text{Np}^{4+}$  to  $\text{NpO}_2^{2+}$  (6). The formal potentials for these reactions are given below in Scheme 2 (6, 8).



**Scheme 2.**

It is important to note that these  $E^\circ$  values are given at 25 °C and 1 atm. Our reactions are occurring at 200 °C and approximately 17 atm (if  $\text{H}_2\text{O}$  exhibits the vapor pressure of pure water), and therefore these potentials can only be used for guidance. These reactions should be thought of as taking place in steam under autogenously generated pressure. There is approximately 170  $\mu\text{L}$  of liquid water present at 200 °C in a reaction that starts with 250  $\mu\text{L}$  of water. In contrast, there will only be 20  $\mu\text{L}$  of liquid water present at 200 °C in a reaction that

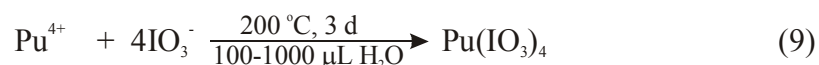
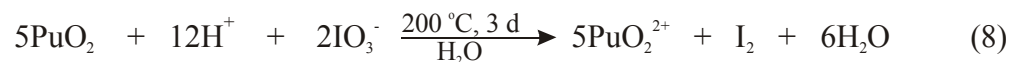
begins with 100  $\mu\text{L}$  of water. When the reactions occur with only a limited amount of liquid water present, as is demonstrated in Reactions 2 and 7, reduction of  $\text{NpO}_2^{2+}$  back to  $\text{Np}^{4+}$  takes place. When sufficient amounts of water are present to approximate a solution (500  $\mu\text{L}$ ), as in Reaction 6, the predicted reaction between  $\text{NpO}_2$  and iodate occurs, via Reaction 2, and  $\text{NpO}_2(\text{IO}_3)_2(\text{H}_2\text{O})$  and  $\text{NpO}_2(\text{IO}_3)_2 \cdot \text{H}_2\text{O}$  form (9). Reaction 5 is the most interesting of this series, and represents conditions under which comproportionation of  $\text{Np}^{4+}$  and  $\text{NpO}_2^{2+}$  occurs to yield two equivalents of  $\text{NpO}_2^+$ . It is important to note that even when the Np(VI) products are isolated as solids, they can be slowly converted to Np(IV) iodates by the application of appropriate hydrothermal conditions (250  $\mu\text{L}$  water), as is shown in Reaction 7. If the amount of water is increased to 500  $\mu\text{L}$ , reduction does not take place.



### Scheme 3.

Reactions 2–5 are not solely driven by the solution phase thermodynamics of the oxidation of  $\text{Np}^{4+}$  by iodate, but also by the reduction of Np(VI) to yield Np(IV), and the subsequent crystallization of the Np(IV) iodate products,  $\text{Np}(\text{IO}_3)_4$  and  $\text{Np}(\text{IO}_3)_4 \cdot n\text{H}_2\text{O}$ . Figure 1 depicts the results of Reaction 7, and shows crystals of  $\text{Np}(\text{IO}_3)_4$  and  $\text{Np}(\text{IO}_3)_4 \cdot n\text{H}_2\text{O}$  that have grown directly off of the surface of delaminating crystals of  $\text{NpO}_2(\text{IO}_3)_2(\text{H}_2\text{O})$ . This result supports that the reaction is a solid-to-solid transformation that is probably surface-mediated. The same may be true for Reactions 2–5. In the presence of a large external radiation source, radiolysis products of water (e.g.  $\text{H}$ ,  $\text{HO}_2$ , and  $\text{H}_2\text{O}_2$ ) might play a role in the reduction of Np(VI) to Np(IV) (10).

As was observed with Np, the reaction of PuO<sub>2</sub> with iodate leads to the two-electron oxidation of Pu<sup>4+</sup> to PuO<sub>2</sub><sup>2+</sup> with concomitant production of elemental iodine (Reaction 8).



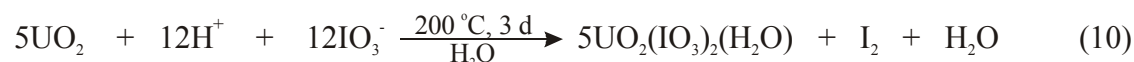
#### Scheme 4.

In contrast to the <sup>237</sup>NpO<sub>2</sub> reactions, the reaction of <sup>242</sup>PuO<sub>2</sub> with iodate with less than 1000 μL of water leads almost solely to the formation of Pu(IO<sub>3</sub>)<sub>4</sub> (11). Reactions with 1000 μL of water produce trace amounts of the Pu(VI) product, PuO<sub>2</sub>(IO<sub>3</sub>)<sub>2</sub>·H<sub>2</sub>O (9,12), but the major product is still Pu(IO<sub>3</sub>)<sub>4</sub>. When 3000 μL of water are used, the only product that is isolated is Pu(IO<sub>3</sub>)<sub>4</sub>. These results imply that the hydrothermal chemistry of Pu iodates is dominated to an even greater extent than in the Np reactions by the formation of the An(IV) iodates.

In previous work it was shown that stock solutions of Pu<sup>4+</sup> and NpO<sub>2</sub><sup>+</sup> react with excess metaperiodate, IO<sub>4</sub><sup>-</sup>, to yield products that contain the actinides in the +6 oxidation state (e.g. NpO<sub>2</sub>(IO<sub>3</sub>)<sub>2</sub>(H<sub>2</sub>O) and AnO<sub>2</sub>(IO<sub>3</sub>)<sub>2</sub>·H<sub>2</sub>O (An = Np, Pu)) (9,12). Metaperiodate contains I(VII), and is a much stronger oxidant than iodate. Clearly, the reactions reported herein of AnO<sub>2</sub> (An = Np, Pu) with iodate under hydrothermal conditions with limited amounts of water are dramatically different from those of aqueous actinide ions with very strong oxidants. While these reactions are occurring at a much lower pH than natural groundwaters, this work calls into question the use of standard solution reactivity data on actinide ions to predict the behavior of SNF that will start off as a reduced solid. The thermodynamic data for actinide complexation are

already being reevaluated in light of the substantial changes that occur at elevated temperatures (13).

The least complex of these reactions is that of  $\text{UO}_2$  with iodate. The process proceeds in accordance with Reaction 10, yielding only U(VI) iodates, such as  $\text{UO}_2(\text{IO}_3)_2(\text{H}_2\text{O})$  (14). Given the ease of oxidation of  $\text{U}^{4+}$  to  $\text{UO}_2^{2+}$ , this result is not surprising (6).



### Scheme 5.

In addition to the new actinide reactivity patterns, these syntheses provide access to single crystals of  $\text{An}(\text{IO}_3)_4$  ( $\text{An} = \text{Np}$  and  $\text{Pu}$ ) and  $\text{Np}(\text{IO}_3)_4 \cdot n\text{H}_2\text{O}$ . The crystal structure of  $\text{An}(\text{IO}_3)_4$  ( $\text{An} = \text{Np}$  and  $\text{Pu}$ ) consists of eight-coordinate, trigonal dodecahedral An(IV) centers ( $D_{2d}$ ) bridged by iodate to form one-dimensional chains as is shown in Figure 2a (15,16). The Np centers reside on  $\bar{4}$  sites yielding two independent An–O bond distances of 2.329(4) Å ( $\times 4$ ) and 2.358(4) Å ( $\times 4$ ) (for  $\text{Np}(\text{IO}_3)_4$ ). The I–O bond distances of 1.782(5), 1.811(4), and 1.827(4) Å are normal (12). The terminal I–O bond distance is slightly shorter than those bridging to the Np(IV) ions. These chains pack together in a pin-wheel fashion (Figure 2b). While the structures of Np(IV) iodates are expected to be similar, if not identical, with those of Th(IV), we have yet to isolate a Th-analog of  $\text{Np}(\text{IO}_3)_4$ , although, the Ce(IV) version can be prepared, which underscores some of the problems of using early, less radioactive actinides like Th(IV) and U(IV) as surrogates for Np(IV) and Pu(IV) (17-19). This was also observed in the An(VI) iodates, where the U(VI) and Pu(VI) compounds are not isostructural (9,12).

$\text{Np}(\text{IO}_3)_4$  crystallizes as single crystals that can have maximum dimensions as large as several millimeters, making this compound amenable to single-crystal magnetic susceptibility measurements. Magnetic susceptibility data for  $\text{Np}(\text{IO}_3)_4$  are shown in Figure 3. Data were collected on two different crystals yielding  $\mu_{\text{eff}}$  of 2.22 and 2.25  $\mu_{\text{B}}$  per Np atom for the different crystals. The observed magnetic moment for the  $\text{Np}^{4+}$  ions in  $\text{Np}(\text{IO}_3)_4$  is markedly lower than that calculated for the free-ions (3.62  $\mu_{\text{B}}$ ) (20). This is not a reflection of covalency of the 5f orbitals, but rather arises from crystal field effects in  $\text{Np}(\text{IO}_3)_4$ , as has also been suggested recently for two Np(V) compounds (21). Magnetic fields well outside of the range of a standard 7 T magnet would be needed to achieve full saturation of the magnetic moment (6). The data follow the Curie-Weiss law with  $\theta = 0.0(5)$  K, indicating that the Np(IV) ions are magnetically isolated from one another. This observation is consistent with the large Np $\cdots$ Np distance of 5.306(1) Å within the one-dimensional chains.

These synthetic, structural, and magnetic data provide new avenues for addressing the reactivity, structures, and properties of transuranic compounds. The use of hydrothermal conditions with smaller amounts of water than has typically been employed gives access to pure compounds in the form of single crystals that have not been previously available from standard synthetic techniques. In a general sense, the actinide chemistry presented here can be considered as being a part of a larger synthetic methodology wherein redox reactions are used to control the introduction of ions that lead to the slow crystallization of highly insoluble products (14b,22). This gradual introduction of reactants facilitates crystal growth of compounds that normally only form microcrystalline or amorphous powders.



## References and Notes

1. a) H. Bruchertseifer, R. Cripps, S. Guentay, B. Jaeckel, *Anal. Bioanal. Chem.* **375**, 1107 (2003). b) Z. Huang, K. Ito, A. R. Timerbaev, T. Hirokawa, T. *Anal. Bioanal. Chem.* **378**, 1836 (2004). c) A. J. Bard, R. Parsons, J. Joseph, *Standard Potentials in Aqueous Solution*, (Dekker, New York, 1985). d) Charlot, G. *Oxidation-Reduction Potentials* (Pergamon, London, 1958). e) Pourbaix, M. *Atlas d'équilibres électrochimiques à 25 °C*, (Gautier Villars, Paris, 1963).
2. M.-J. Crawford, A. Ellern, K. Karaghiosoff, P. Mayer, H. Noth, M. Suter, M. *Inorg. Chem.* **43**, 7120 (2004).
3. a) G. R. Choppin, F. I. Khalili, E. N. Rizkalla, *J. Coord. Chem.* **26**, 243 (1992). b) P. R. V. Rao, S. K. Patil, *Radiochem. Radioanal. Lett.* **36**, 169 (1978).
4. a) G. T. Seaborg, A. C. Wahl, *J. Am. Chem. Soc.* **70**, 1128 (1948). b) B. B. Cunningham, L. B. Werner, *J. Am. Chem. Soc.* **71**, 1521 (1949). c) G. T. Seaborg, S. G. Thompson, U.S. Patent #2,950,168 (1960).
5. M. Kaholek, L. Triendl, *React. Kinet. Catal. Lett.* **63**, 297 (1998).
6. a) L. R. Morss, N. M. Edelstein, J. Fuger, *The Chemistry of the Actinide and Transactinide Elements* (Springer, Heidelberg, 2006). b) J. J. Katz, G. T. Seaborg, L. R. Morss, *The Chemistry of the Actinide Elements* (Chapman and Hall, New York, ed 2, 1986).
7. *Syntheses*. UO<sub>2</sub> (99.8%, Alfa Aesar, depleted), <sup>237</sup>NpO<sub>2</sub> (99.9%, Oak Ridge, t<sub>1/2</sub> = 2.14 × 10<sup>6</sup> y), <sup>242</sup>PuO<sub>2</sub> (99.9%, Oak Ridge, t<sub>1/2</sub> = 3.76 × 10<sup>5</sup> y), and HIO<sub>3</sub> (99.5%, Alfa Aesar) were used as received. Distilled and Millipore filtered water with a resistance of 18.2 MΩ·cm was used in all reactions. Reactions were run in Parr 4749 autoclaves with

custom-made 10-mL PTFE liners. All reactions were conducted with 10 mg of AnO<sub>2</sub> (An = U, Np, or Pu) and a tenfold molar excess of iodic acid unless otherwise noted. Sealed reaction vessels were placed in box furnaces that had been pre-heated to 200 °C. The reaction are occurring under an air atmosphere. Cooling was accomplished by turning the furnaces off.

8. D. R. Lide, *CRC Handbook of Chemistry and Physics*, 71<sup>st</sup> Ed. (CRC Press, Boston, 1990).
9. A. C. Bean, B. L. Scott, T. E. Albrecht-Schmitt, W. Runde, *Inorg. Chem.* **42**, 5632 (2003).
10. M. V. Vladimirova, *Radiochem.* 39, 250 (1997).
11. As a cautionary note, both Np(IO<sub>3</sub>)<sub>4</sub> and Pu(IO<sub>3</sub>)<sub>4</sub> are pleochroic owing to their low-dimensional structures. Different crystal growth conditions leads to changes in crystal morphology, agglomeration of crystallites, and different product coloration depending on the angle that the crystallites are viewed. For Np(IO<sub>3</sub>)<sub>4</sub>, grey to green to black transitions can be observed by rotating single crystals and clusters of crystals; whereas for Pu(IO<sub>3</sub>)<sub>4</sub>, blue to green to brown coloration is exhibited. Crystals of Np(IO<sub>3</sub>)<sub>4</sub>·nH<sub>2</sub>O have a very pale yellow coloration.
12. W. Runde, A. C. Bean, T. E. Albrecht-Schmitt, B. L. Scott, *Chem. Commun.* **4**, 478 (2003).
13. L. Rao, T. G. Srinivasan, A. Y. Garnov, P. L. Zanonato, P. Di Bernardo, A. Bismondo, *Geochim. Cosmochim. Acta* **68**, 4821 (2004).
14. a) F. Weigel, L. W. H. Engelhardt, *J. Less-Common Met.* **91**, 339 (1983). b) A. C. Bean, S. M. Peper, T. E. Albrecht-Schmitt, *Chem. Mater.* **13**, 1266 (2001).

15. Crystallographic data for **Np(IO<sub>3</sub>)<sub>4</sub>**: grey-green-black octagonal bipyramid, dimensions 0.182 x 0.133 x 0.106 mm, tetragonal,  $P4_2/n$ ,  $Z = 2$ ,  $a = 9.8790(5)$ ,  $c = 5.3063(4)$  Å,  $V = 517.87(5)$  Å<sup>3</sup> ( $T = 193$  K),  $\mu = 220.17$  cm<sup>-1</sup>,  $R_1 = 0.0250$ ,  $wR_2 = 0.0654$ . **Pu(IO<sub>3</sub>)<sub>4</sub>**: blue prism, 0.039 x 0.008 x 0.008 mm, tetragonal,  $P4_2/n$ ,  $Z = 2$ ,  $a = 9.869(1)$ ,  $c = 5.2861(7)$  Å,  $V = 514.8(1)$  Å<sup>3</sup> ( $T = 193$  K),  $\mu = 184.57$  cm<sup>-1</sup>,  $R_1 = 0.0266$ ,  $wR_2 = 0.0467$ . Bruker APEX CCD diffractometer:  $\theta_{\max} = 56.62^\circ$  ( $56.50^\circ$  for Pu), MoK $\alpha$ ,  $\lambda = 0.71073$  Å,  $0.3^\circ$   $\omega$  scans, 4357 (4925 for Pu) reflections measured, 630 (637 for Pu) independent reflections all of which were included in the refinement. The data was corrected for Lorentz-polarization effects and for absorption (numerical and multiscan), the structure was solved by direct methods, followed by a refinement of  $F^2$  by full-matrix least-squares with 40 parameters. G. M. Sheldrick, SHELXTL NT/2000, Version 6.1, Bruker AXS, Inc.: Madison, WI 2000.
16. Some crystallographic details for **Np(IO<sub>3</sub>)<sub>4</sub>·nH<sub>2</sub>O**: pale yellow needles, rhombohedral,  $R3c$ ,  $Z = 18$ ,  $a = 21.868(1)$ ,  $c = 12.9705(8)$  Å,  $V = 5371.4(5)$  Å<sup>3</sup> ( $T = 193$  K). The acentricity of the structure was confirmed by second-harmonic generation measurements on the Th-analog of Np(IO<sub>3</sub>)<sub>4</sub>·nH<sub>2</sub>O.
17. a) T. A. Sullens, P. M. Almond, T. E. Albrecht-Schmitt, *Mater. Res. Soc.* **893**, 283 (2006). b) A. E. V. Gorden, D. K. Shuh, B. E. F. Tiedemann, R. E. Wilson, J. Xu, K. N. Raymond, *Chemistry*, **11**, 2842 (2005).
18. A historical footnote is worthwhile here: The microscale precipitation of Pu(IO<sub>3</sub>)<sub>4</sub> was used by B. B. Cunningham and L. B. Werner to show, for the first time, that Pu has a stable +4 oxidation state in 1942 (3b). Since this time Pu(IO<sub>3</sub>)<sub>4</sub> has been used as a benchmark compound because of its remarkable insolubility in low pH media. The

structure, precise elemental analyses, and spectroscopic data for Pu(IV) iodates has never been reported in the primary literature. We believe that the compound referred to in the past as  $\text{Pu}(\text{IO}_3)_4$  is in fact  $\text{Pu}(\text{IO}_3)_4 \cdot n\text{H}_2\text{O}$ , and not the anhydrous  $\text{Pu}(\text{IO}_3)_4$ .

19. Staritsky, E.; Cromer, D. T. *Anal. Chem.* 28, 913 (1956).
20. C. Kittel, *Introduction to Solid State Physics*, 6<sup>th</sup> Ed., (Wiley, New York, 1986).
21. T. Z. Forbes, P. C. Burns, L. Soderholm, S. Skanthakumar, *Chem. Mater.* 18, 1643 (2006).
22. See for example: D. Grohol, K. Matan, J.-H. Cho, S.-H. Lee, J. W. Lynn, D. G. Nocera, Y. S. Lee, *Nature Materials*, 4, 323 (2005).
23. We are grateful for support provided by the Office of Civilian Radioactive Waste Management, Office of Science and Technology and International, through a subcontract with Argonne National Laboratory, and by the Chemical Sciences, Geosciences, and Biosciences Division, Office of Basic Energy Sciences, Office of Science, Heavy Elements Program, U.S. Department of Energy, under Grant DE-FG02-01ER15187, and under Contracts W-31-109-ENG-38 at Argonne National Laboratory, and Contract DE-AC05-00OR22725 with Oak Ridge National Laboratory, managed by UT-Battelle, LLC. JSB and ESC acknowledge support from NSF-DMR 0203532. A portion of this work was performed at the National High Magnetic Field Laboratory, which is supported by the National Science Foundation Cooperative Agreement No. DMR-0084173, by the State of Florida, and by the Department of Energy.

## Figure Captions

- Figure 1.** A photograph showing the hydrothermal reduction of the Np(VI) iodate,  $\text{NpO}_2(\text{IO}_3)_2(\text{H}_2\text{O})$ , to the Np(IV) iodates,  $\text{Np}(\text{IO}_3)_4$  and  $\text{Np}(\text{IO}_3)_4 \cdot n\text{H}_2\text{O}$ .
- Figure 2.** a) A view of the one-dimensional chains in  $\text{An}(\text{IO}_3)_4$  ( $\text{An} = \text{Np}$  and  $\text{Pu}$ ) consisting of eight-coordinate, dodecahedral An(IV) centers bridged by iodate.  
b) A depiction of the pin-wheel packing of the  $\text{An}(\text{IO}_3)_4$  chains.
- Figure 3.** The temperature dependence of magnetic moment and molar susceptibility (inset) of a  $\text{Np}(\text{IO}_3)_4$  single crystal. The Curie-Weiss fitting curve is also shown as a solid line in the inset.